

ResDepth: Learned Residual Stereo Reconstruction

Corinne Stucker Konrad Schindler

Photogrammetry and Remote Sensing, ETH Zurich

{firstname.lastname@geod.baug.ethz.ch}

Abstract

We propose an embarrassingly simple, but very effective scheme for high-quality dense stereo reconstruction: (i) generate an approximate reconstruction with your favourite stereo matcher; (ii) rewrap the input images with that approximate model; and (iii) with the initial reconstruction and the warped images as input, train a deep network to enhance the reconstruction by regressing a residual correction. The strategy to only learn the residual greatly simplifies the learning problem. A standard Unet without bells and whistles is enough to reconstruct even small surface details, like dormers and roof substructures in satellite images. We also investigate residual reconstruction with less information and find that even a single image is enough to greatly improve an approximate reconstruction. Our full model reduces the mean absolute error of state-of-the-art stereo reconstruction systems by $>50\%$, both in our target domain of satellite stereo and on stereo pairs from the ETH3D benchmark.

1. Introduction

Dense stereo reconstruction is a classical task of computer vision with a rich history and an elementary building block of 3D perception. The problem statement is simple: given two images with overlapping fields of view and known relative pose, find a 3D scene that is photo-consistent with both views. Efficient solutions exist and form the basis for a wide range of operational systems, ranging from large-scale topographic reconstruction to industrial machine vision and mobile robotics.

Maximising photo-consistency across all pixels is, however, not enough to solve dense stereo. Rather, one must also impose a suitable prior on the 3D scene. Classical stereo algorithms [13, 10] typically include an explicit preference for piece-wise smooth surfaces. Since that prior is rather unspecific and knows very little about the structure of the observed scene, the resulting surface models must in practice still be cleaned up. E.g., in topographic mapping, it

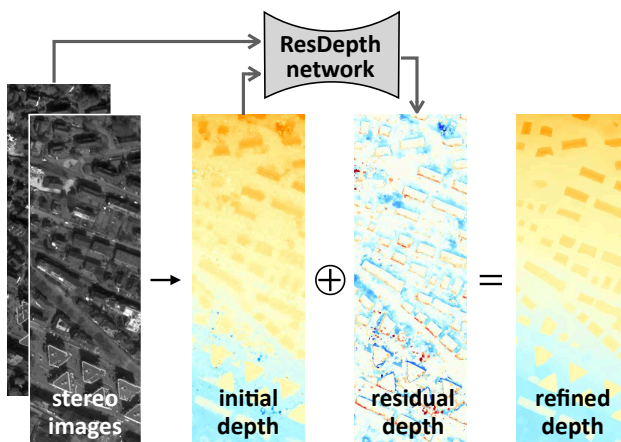


Figure 1. Instead of learning stereo reconstruction from scratch, our *ResDepth* network is trained to refine an initial depth (respectively, height) map with the help of stereo images. Our main message is that this residual correction is a lot easier to learn.

is common to enhance building shapes with heuristic rules; in mobile robotics, reflecting glass must be detected and cleaned up in post-processing; *etc.*

The need to capture complex, soft prior expectations about the world, which are hard to formulate explicitly, naturally fits a machine learning approach. Indeed, several authors have recently proposed to learn stereo matching, i.e., design a deep encoder-decoder network that maps the input images to a depth map. We argue that, while conceptually elegant, such a purely learning-based solution may be inefficient because it has to learn a lot of things from data that are already well captured by existing stereo methods. Importantly, classical stereo matching algorithms are very robust in the sense that their outputs are usually correct as a coarse, *global* estimate of the scene surface but may suffer from *local* biases and errors. Their main shortcoming is a lack of prior knowledge about the observed world beyond simplistic (piece-wise) smoothness.

1.1. Contribution

We advocate a *residual learning* strategy: we leave the reconstruction of an approximate surface to a standard stereo matcher that may have certain biases but robustly produces passable stereo models. We then train a deep network to upgrade that initial estimate, see Fig. 1. In this way, the network has access not only to the images but also to the initial surface model and can concentrate on the part of the problem for which it is most needed: its task becomes to intervene where the assumptions built into the initial stereo algorithm fail and a more intricate prior is needed that must be learned from data. Intuitively, learning an additive update that is mostly small is easier than learning the entire depth estimation process – this is just another of the ubiquitous optimisation strategy to start from an approximate solution and refine it. Moreover, it is also easier to choose the right prior locally for a specific region whose 3D geometry is already roughly known (e.g., a house-sized protrusion in a city model is a strong indication that the surface might conform to a common roof shape, see Fig. 2). Finally, the proposed approach makes it easy to tune the reconstruction to the user’s needs. E.g., one can train *ResDepth* to remove trees from the surface model simply by supervising it with a city model without trees. Such a filter would be a lot more difficult to construct without an initial reconstruction to guide both tree detection and ”inpainting” of the correct ground height. An alternative interpretation of our method is as a learned enhancement filter for depth maps guided by the original image content.

Technically, the proposed approach can be implemented as follows: (i) reconstruct an initial depth map with some stereo matcher – we use a conventional one, but it could be a learned one too; (ii) project the two images onto the depth map – note that the resulting synthetic images will be photo-consistent wherever the depth map is correct; (iii) feed the depth map together with the projected images to a neural network that predicts an additive residual correction of the depth map. (iv) if desired, iterate the refinement with the new, improved depth map.

We find that this simple scheme greatly improves the reconstructed 3D depth. The improvement is particularly noticeable for scenes with small, high-frequency surface structures (relative to the pixel size), for instance buildings in satellite images. In our experiments, *ResDepth* achieves a $2.5\times$ reduction of the median error compared to conventional satellite stereo reconstruction.

2. Related work

2.1. Conventional stereo matching

Classical stereo methods boil down to finding a dense set of correspondences that have high photo-consistency, while at the same time forming a (piece-wise) smooth surface.

Algorithmically, the key issue is to find efficient approximations for the smoothness prior using for instance graph cuts [13], dynamic programming [10] or the PatchMatch method [5]. To handle high-resolution images, e.g., in aerial mapping, these methods are often employed iteratively in a spatial pyramid scheme [20], whose later iterations can be seen as a refinement of a coarser initial solution. Other stereo algorithms are by design iterative, including many variational schemes [22, 1] and methods based on mesh surfaces [15].

2.2. Deep stereo matching

In the last few years, the focus has been on stereo methods that harness the power of deep learning. While early attempts only learned to measure patch similarity within a conventional optimisation [28], more recent methods use encoder-decoder architectures to directly output disparity maps [17, 6]. Some of the latest methods can also handle high-resolution images [25, 27]. Most closely related to our work are recent, rather complex stereo architectures that internally split the computation into a first, coarse disparity estimation and a subsequent refinement [18, 16]. We argue that this may not be necessary: the critical step for high-quality reconstructions appears to be the learned refinement, which can be accomplished with a simple standard architecture that needs much less training data; to initialise it, standard stereo methods are sufficient.

2.3. Filtering and refinement of depth maps

A number of works have looked at ways to improve an initial 3D surface. [26, 4] iteratively deform a surface mesh to maximise photo-consistency, whereas [7] aim to detect regions of incorrect disparity and relabel them, guided by a single image. In the context of topographic mapping, it is common to refine buildings by fitting parametric models [8, 14]. More recently, it has been proposed to learn a general prior for enhancing digital elevation models [2], including a version guided by an ortho-image [3].

3. Method

Our goal is dense surface reconstruction by stereo matching. Hence, we start from images with overlapping field of view and known camera pose. For simplicity, the following explanations assume a binocular stereo setup, note however that extending *ResDepth* to a fixed number of views ≥ 2 is straight-forward by simply adding input channels to the network.

3.1. Initial reconstruction

Besides the input images, *ResDepth* requires a coarse initial reconstruction. To play to the strength of convolutional networks, that reconstruction should be parametrised

over a regular 2D grid. We distinguish two cases. For the case of aerial or satellite imaging, a natural choice is a digital elevation model (DEM), i.e., a raster of height values along the gravity axis. Here, we use a DEM generated with a re-implementation of state-of-the-art hierarchical semi-global matching [20]. For close-range images, the reconstruction is represented as a depth map in the camera coordinate system of one of the views. Our depth maps are generated with the PatchMatch stereo [5] implementation of COLMAP [21].

3.2. Image rectification

For further processing in *ResDepth*, the images should be aligned with the depth map. This is achieved by rewarping them. In the satellite case, this corresponds to independently ortho-rectifying the images. In the close-range case, it is a texture remapping from the second image to the reference camera used to parametrise the depth map. Note that this rewarping compensates the influence of the viewing geometry to an even greater extent than epipolar rectification: the disparities in the warped images are, by construction, small everywhere except at large depth errors. No model capacity is wasted to learn stereo reconstruction across a wide range of permissible disparities.

If the reconstruction were perfect, the two images would be perfectly aligned after the warping, and hence maximally photo-consistent. Thus, discrepancies between the two warped images provide a signal of how to improve the depth. The only regions where a correct depth map would not achieve photo-consistency are those that are occluded in one view. In such cases, we nevertheless project the image texture, i.e., we do not z -buffer correctly but prefer to render duplicate textures if the corresponding rays intersect the surface twice. The rationale is that the very systematic patterns generated in this way – not photo-consistent, systematically displaced copies of nearby textures – provide even stronger evidence about the surface shape than empty pixels.

3.3. ResDepth network

In terms of network architecture, we found that a fairly standard Unet [19] works well. We use 5 levels for satellite images (input patch size 128×128), see Tab. 1. For close-range images (input patch size 512×512), we use 7 levels, such that in both cases the bottleneck has dimensions $512 \times 4 \times 4$. Each encoder level consists of the sequence 3×3 conv – batch norm – ReLU – 2×2 max pool. The decoder levels are similar, except that max-pooling is replaced by up-convolution with stride $\frac{1}{2}$. All inputs are simply stacked into a single multi-channel image and fed to the network.

The main motivation for our residual stereo method is to reconstruct crisp crease edges and depth discontinuities and to align them with the image content. In that context, an

input 3,128,128	→	output 1,128,128
conv/bn/relu/maxpool 64,64,64	→	upconv/conv 64,64,64
conv/bn/relu/maxpool 128,32,32	→	upconv/conv/bn/relu 128,32,32
conv/bn/relu/maxpool 256,16,16	→	upconv/conv/bn/relu 256,16,16
conv/bn/relu/maxpool 512,8,8	→	upconv/conv/bn/relu 512,8,8
		conv/bn/relu 512,4,4

Table 1. *ResDepth-stereo* architecture for satellite images. For close-range data, we add two additional levels to account for the larger input patch size.

important feature of a Unet-type architecture is the exhaustive set of skip connections from encoder to decoder levels of the same resolution, which make sure no high-frequency detail is lost. Recall that in our case we add a long residual connection that directly adds the input depth to the output of the last Unet layer, so that the network only learns what must be added to the input depth to get to the ground truth.

The network is trained in a fully supervised manner by minimising the pixel-wise absolute distance to ground truth depth maps (i.e., the ℓ_1 -loss).

3.4. Implementation details

For the satellite case, we train the network with 128×128 pixel patches (32×32 m in world coordinates), which we randomly crop from the training region. The network is trained with ADAM with base learning rate 10^{-5} , batch size 20, and weight decay of 10^{-5} . For the close-range scenario, where much larger windows are needed to capture context, we use 512×512 pixel patches that are randomly cropped from all images of our training set. We again optimise with ADAM with base learning rate 10^{-5} , batch size 4, and weight decay of 10^{-5} .

3.5. Network variants

As mentioned, our method can be regarded as an image-guided depth enhancement filter. That view leads to the question of how much each input channel contributes, and whether all inputs are indeed needed to achieve the desired effect. Moreover, there may be situations where not all inputs are available, e.g., one may be faced with the task of improving an existing DEM for which one has access to a single image only, but not to stereo coverage.

With the proposed framework it is straight-forward to construct several potentially interesting variants, respec-

	Overall			Building pixels only			Non-building pixels only		
	MAE	RMSE	MedAE	MAE	RMSE	MedAE	MAE	RMSE	MedAE
Initial DEM	3.85	5.89	1.92	2.84	4.67	1.37	4.30	6.37	2.40
Median filtered	2.91	4.67	1.42	2.73	4.47	1.36	3.00	4.78	1.48
Unet- <i>stereo</i>	7.54	9.23	6.10	8.36	9.85	7.72	7.17	8.93	5.39
ResDepth- <i>0</i>	1.71	3.36	0.71	2.47	4.62	0.86	1.38	2.63	0.65
ResDepth- <i>mono</i>	1.43	2.82	0.62	1.86	3.73	0.65	1.25	2.31	0.60
ResDepth- <i>stereo</i>	1.33	2.67	0.57	1.75	3.63	0.57	1.15	2.11	0.57
ResDepth- <i>stereo-iter</i>	1.28	2.67	0.54	1.79	3.73	0.59	1.06	2.03	0.52

Table 2. Quantitative results on Zurich data, in metres. Residuals beyond ± 20 m were discarded before computing statistics to account for temporal changes between ground truth and images; building masks for object-specific metrics were dilated by 2 pix (0.5 m) to avoid aliasing at vertical walls.

tively baselines. Starting from the configuration described so far, which we refer to as ResDepth-*stereo*, the following simplifications are possible:

ResDepth-*mono* does not use the second input image, similar to [3]. Therefore, it has no access to stereo disparities but can still use the monocular image information to enhance the depth map. Potentially, this includes both low-level and high-level information. Low-level image edges may serve to sharpen and localise depth edges and jumps, in the spirit of the guided filter [9]. High-level information implicit in the image like semantics and layout can also be valuable, e.g., it may serve to distinguish large trees from small buildings.

ResDepth-*0* does not use any image information at all. It merely learns a prior on the structure of depth images and corrects unlikely configurations of depth values without conditioning on image evidence, as in [2]. In the above analogy, it can be thought of as a sort of clever, learned bilateral filter [24] with the additional capability to recognise and exploit long-range correlations such as straight gable lines.

In the opposite direction, one can also design more sophisticated variants. One obvious idea that we have not yet tested is to build a ResDepth-*multiview*. As long as the number of input views is fixed, one could warp more than two images and stack them into the network input. Given the binocular results (see Sec. 4), we expect at most small, and diminishing, improvements when adding further views.

An interesting extension is to iterate the residual correction. ResDepth-*stereo-iter* uses the output depth of ResDepth-*stereo* as input, warps the input images with the new, improved depth map, and trains another ResDepth-*stereo* network to further reduce the new, smaller depth errors. This iterative optimisation yields only small quantitative gains, but visibly sharper and more detailed 3D geometry, see Fig. 2. We note that, in principle, it is possible to concatenate the two iterations and train them end-to-end,

since the image warping is differentiable. While certainly more elegant, it is unlikely that doing so will in practice lead to better results. It has been reported that in some applications weights can be shared across unrolled network iterations [12]. We plan to explore that option in future work.

4. Experimental evaluation

We have evaluated the proposed ResDepth method in two different settings, large-scale urban modelling from high-resolution satellite data and close-range depth estimation on indoor scenes from the high-resolution multi-view ETH3D benchmark dataset [23]. On the satellite data, we also perform an ablation study to assess the influence of different inputs on the reconstruction result.

4.1. Urban DEM refinement

Our main application is 3D city modelling from satellite images. We use a stereo image pair acquired over the area of Zurich/Switzerland between 2014 and 2018 with DigitalGlobe’s WorldView2 satellite. As usual in satellite imaging, only the panchromatic channel is used for reconstruction, since it is recorded at higher resolution (ground sampling distance of 0.46 m at nadir). The initial DEM was produced with an implementation of tSGM, with a grid spacing of 0.25 m. The DEM covers an area of approximately 1.5×1.5 km², including industrial and residential areas. For the evaluation, we vertically split the area into 5 mutually exclusive strips and use 3 strips for training, one for validation, and one for testing. Terrain heights are globally normalised by centering to mean height 0 and scaling by the global standard deviation of the heights. To increase the amount of training data and avoid biases due to the topography (sloped, south-facing terrain), we perform data augmentation by randomly rotating training patches with $\alpha \in \{90^\circ, 180^\circ, 270^\circ\}$ as well as horizontal and vertical flipping.

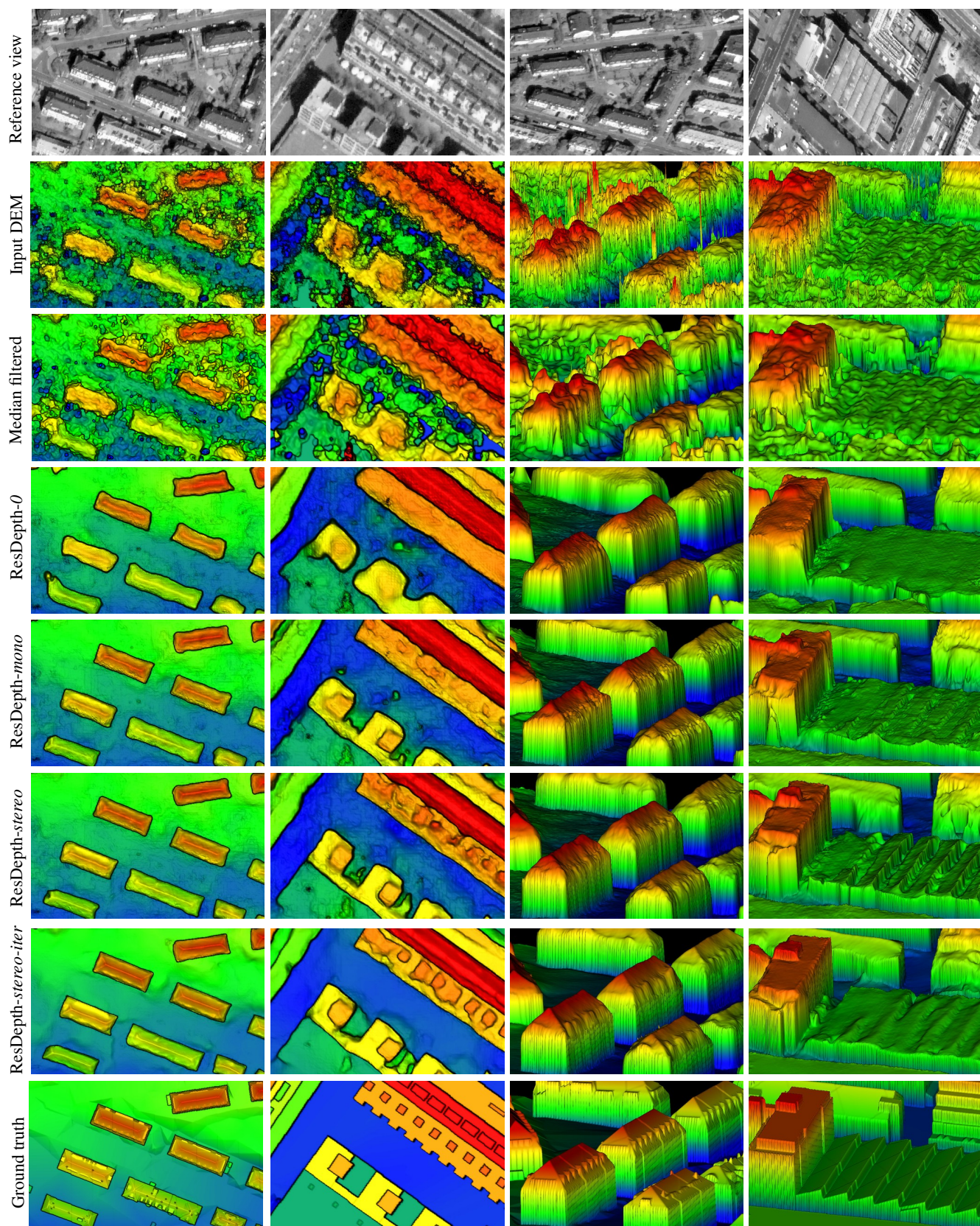


Figure 2. Example results for Zurich with different ResDepth variants.

As ground truth we use the publicly available city model of Zurich¹. That model was assembled semi-automatically by merging airborne laser scans, building and road boundaries (including bridges) from national mapping data, and roof models derived by interactive stereo digitisation. The height accuracy is specified as ± 0.2 m on buildings and ± 0.4 m on general terrain. The model is based on data collected before 2015, due to recent construction it differs from the state visible in the images in a handful of places. The DEM does (deliberately) not contain trees, therefore ResDepth learns to also filter out trees present in the initial model. The initial DEM generated with a dedicated satellite stereo pipeline has a mean absolute error (MAE) of 3.85 m and a median absolute error (MedAE) of 1.92 m, see Tab. 2. For completeness, we also show root mean square errors (RMSEs) in the table, which are generally between $1.5\times$ and $2\times$ higher than MAEs because of outliers, but follow the same trend. Example regions from the DEM are shown in Fig. 2. The DEM is rather noisy. The comparatively high noise level is typical for satellite-derived models due to the limited sensor resolution, the large sensor-to-object distance, and the image quality.

As a baseline for a "cleaned" DEM, we follow a popular strategy implemented in a number of reconstruction packages for satellite and aerial images and apply a median filter (kernel size of 5×5) to denoise the depth map without blurring discontinuities. This does decrease the MAE by almost a metre, but except for removing a few spikes (probably due to mismatches on vegetation) it has little visual effect. As a sanity check for the claim that residual depth is much easier to learn, we also train the ResDepth architecture without the initial DEM as input. I.e., the Unet is fed only the two warped images and trained to output the full depth map. Note that for simplicity we use the same warping as for ResDepth with the initial DEM. Thus, the task is in fact easier than stereo matching from scratch. This test (termed Unet-*stereo*) fails completely, with a MAE of 7.5 m. This means that with the same encoder-decoder architecture and the same amount of training data as used for ResDepth, it is not possible to learn full stereo matching from only images to a depth map.

We then test various variants of ResDepth. As expected, the simple ResDepth-0 without any image evidence mostly acts as a context-aware, intelligent smoothing filter. Notably, it is already much better than the median filter baseline, reducing the MAE to 1.7 m and the MedAE to 0.7 m. Among others, it has learned a preference for vertical walls. Naturally, it is not able to add details missed by the original stereo matcher. Moreover, building outlines remain wobbly, and roofs are blobby or sagging (1st-3rd column in Fig. 2). Next comes ResDepth-*mono*. The combination of a coarse

	Depth-stereo pairs	ResDepth- <i>stereo</i>		COLMAP (unfilt.)	
		MAE	RMSE	MAE	RMSE
Delivery area	4	0.21	0.71	0.24	0.94
Kicker	4	0.15	0.38	0.41	1.11
Office	3	0.14	0.23	0.55	1.21
Pipes	3	0.21	0.61	0.45	1.30
Relief	4	0.19	0.80	0.28	1.11
Relief_2	4	0.12	0.63	0.17	0.52
Terrains	4	0.06	0.17	0.45	1.42
Overall	26	0.15	0.56	0.35	1.13

Table 3. Quantitative results on ETH3D indoor scenes, in metres. Residuals beyond ± 10 m were discarded before computing statistics, since they usually occur only outside of the stereo overlap (for ResDepth and also, in even more extreme form, for COLMAP).

initial DEM with a single image works surprisingly well. Apparently, even without stereo observations, the correlation between intensity patterns in the image and depth patterns in the reconstruction contains a lot of useful information. Substructures on roofs emerge that were not visible in the input DEM, and straight lines and rectangular footprints are more faithfully reproduced. The MAE drops by a further 0.3 m compared to ResDepth-0. We speculate that also in other (learned or hand-crafted) pipelines that iteratively refine the reconstruction, a large portion of the improvement in later processing stages might come from this monocular "transfer" of crisp image structures, rather than from actual stereo correspondence.

Still, ResDepth-*stereo* is able to further improve the reconstruction. Visually, the difference is in fact larger than suggested by the quantitative improvement of a further 0.1 m in MAE, as building shapes become crisper and additional roof details emerge. This trend continues for ResDepth-*stereo-iter*: the edges are visible sharper and straighter, even small dormers are discernible and spurious bumps on roads disappear. Uncommon building structures are sometimes over-smoothed (e.g., the saw-tooth roof in Fig. 2, 4th column), probably because they are not represented in the training data. The final MedAE of our best result after two rounds of ResDepth is about 0.5 m, the MAE is 1.3 m. These values are quite remarkable given the image resolution of ≈ 0.5 m and the uncertainty of the satellite poses on the order of 0.5 m on the ground.

4.2. ETH3D

We also test ResDepth on close-range stereo pairs from the ETH3D dataset. For the experiment, we downsample the images to a size of 886×590 pixels, remove radial distortion, and convert them to gray-scale. We limit ourselves to indoor scenes, and manually pick a set of binocular stereo

¹https://www.stadt-zuerich.ch/ted/de/index/geoz/geodaten_u_plaene/3d_stadtmodell.html

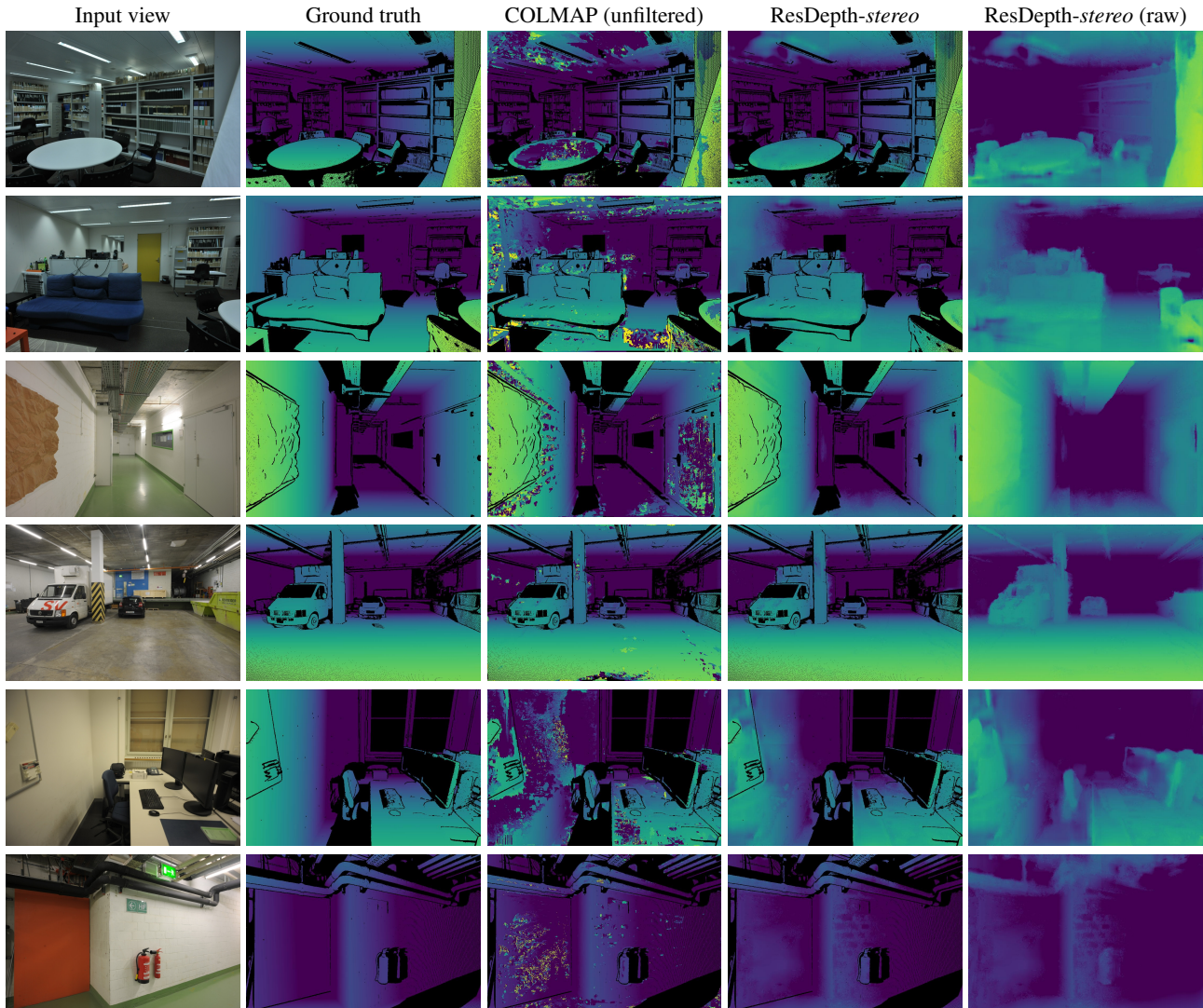


Figure 3. Example results for ETH3D indoor scenes. Pixels without valid ground truth depth are displayed in black (except in the rightmost column, which shows the unmasked ResDepth prediction).

pairs with high overlap and reasonable baselines. The data is split into training, validation, and test portions such that their fields of view are mutually exclusive, i.e., scene part visible in the test set are never seen in the training or validation part. Initial depth maps were generated with the Patch-Match implementation of COLMAP. Because of the much larger depth range (relative to the baseline), we operate in inverse depth, i.e., pixel-wise depth values d are converted to $1/d$ for training and prediction. The ResDepth-*stereo* network is trained on patches of size 512×512 cropped randomly from all training images. Gray-values are normalised to $[0 \dots 1]$, inverse depth values are centred to the mean inverse depth of the patch. Patches are horizontally flipped at random for data augmentation.

The ground truth depth maps for ETH3D are given in the thin-prism fisheye camera model of the original images. We undistort and downsample them to 886×590 to match the images. As baseline, we compare to the dense matcher of COLMAP, with heuristic filtering turned off in order to obtain dense depth maps. For the evaluation, we convert back to metric depth, on the one hand because this is our target quantity, and on the other hand because inverse depths are not comparable between stereo pairs with different baselines.

The ETH3D ground truth has been acquired with a surveying-grade laser scanner and has missing values in some regions due to occlusions, specular reflections, dark surfaces, *etc.* During both training and evaluation, deviations from ground truth can only be measured at valid

ground truth points. To give a correct impression where quantitative differences originate, we therefore mask out pixels without ground truth in all depth maps in Fig. 3. For reference, we also show the unmasked maps produced by ResDepth in the rightmost column.

As can be seen in Tab. 3, ResDepth consistently improves over the COLMAP baseline, in some scenes considerably. On average, the MAE is decreased from 0.35 m to 0.15 m. While the quantitative results are very encouraging, the visual impact of ResDepth is smaller in the close-range scenario. In the urban modelling case, both the images and the ground truth DEM contain a lot of structure that it can learn to exploit, like building shapes, roof lines, trees, *etc.* On the contrary, objects in the close-range images are much larger (relative to the pixel size), there are few sharp discontinuities, and the prevalent structure even over fairly large local neighbourhoods is planarity. ResDepth does manage to recover quite a bit of detail that is incorrect in the COLMAP input, such as the chairs in the 1st row of Fig. 3 and the area around the sofa in the 2nd row. But one of the main drivers of its good performance appears to be that it has learned the sensible, if unspectacular prior to associate featureless, homogeneous image regions with planar surfaces. In Fig. 3 for instance, the table in the 1st row, the floor in the 2nd row, the wall in the 3rd row. We point out that the stereo matching is evaluated in isolation, at completeness 100%, as suggested in [11]. That comparison should be taken with a grain of salt: most of the error of COLMAP is due to areas that are masked out if its internal filter is switched on. I.e., COLMAP is aware of the problems and would discard them if permitted, at the cost of lower completeness.

5. Conclusion

We have presented an astonishingly simple, yet highly effective way to use deep networks for dense 3D reconstruction: instead of replacing existing (hand-crafted or learned) stereo matchers with a deep network, we complement them. The network receives as input both an initial depth map (respectively, height map) and the stereo images, and estimates a depth map that is added to the initial one to improve it. We have shown that with this strategy we can reduce the errors of state-of-the-art stereo matchers by more than 2 \times , with a standard Unet architecture without any special modifications and a moderate amount of training data.

In future work, we plan to test the ResDepth idea also for multi-view stereo, which is straightforward since all views are warped to the same image coordinate system. Furthermore, we believe that it may be possible to train ResDepth in such a way that it can gradually refine the reconstruction over multiple iterations, with the same set of weights.

At a meta-level, we see ResDepth as a reminder to keep things simple, and a strong baseline that should not be overlooked when designing more sophisticated stereo networks.

Acknowledgements

Supported by the Intelligence Advanced Research Projects Activity (IARPA) via Department of Interior / Interior Business Center (DOI/IBC) contract number D17PC00280. The U.S. Government is authorized to reproduce and distribute reprints for Governmental purposes notwithstanding any copyright annotation thereon. Disclaimer: The views and conclusions contained herein are those of the authors and should not be interpreted as necessarily representing the official policies or endorsements, either expressed or implied, of IARPA, DOI/IBC, or the U.S. Government.

References

- [1] Rami Ben-Ari and Nir Sochen. Variational stereo vision with sharp discontinuities and occlusion handling. *ICCV*, 2007.
- [2] Ksenia Bittner, Pablo dAngelo, Marco Körner, and Peter Reinartz. DSM-to-LoD2: Spaceborne stereo digital surface model refinement. *Remote Sensing*, 10(12), 2018.
- [3] Ksenia Bittner, Marco Körner, and Peter Reinartz. DSM building shape refinement from combined remote sensing images based on WNet-cGANs. *arXiv preprint arXiv:1903.03519*, 2019.
- [4] Maros Blaha, Mathias Rothermel, Martin R. Oswald, Torsten Sattler, Audrey Richard, Jan D. Wegner, Marc Pollefeys, and Konrad Schindler. Semantically informed multiview surface refinement. *ICCV*, 2017.
- [5] Michael Bleyer, Christoph Rhemann, and Carsten Rother. PatchMatch stereo-stereo matching with slanted support windows. *BMVC*, 2011.
- [6] Jia-Ren Chang and Yong-Sheng Chen. Pyramid stereo matching network. *CVPR*, 2018.
- [7] Spyros Gidaris and Nikos Komodakis. Detect, replace, refine: Deep structured prediction for pixel wise labeling. *CVPR*, 2017.
- [8] Norbert Haala, Claus Brenner, and Christian Stätter. An integrated system for urban model generation. *ISPRS Archives*, 32:96–103, 1997.
- [9] Kaiming He, Jian Sun, and Xiaoou Tang. Guided image filtering. *ECCV*, 2010.
- [10] Heiko Hirschmüller. Accurate and efficient stereo processing by semi-global matching and mutual information. *CVPR*, 2005.
- [11] Po-Han Huang, Kevin Matzen, Johannes Kopf, Narendra Ahuja, and Jia-Bin Huang. DeepMVS: Learning multi-view stereopsis. In *CVPR*, 2018.
- [12] Junhwa Hur and Stefan Roth. Iterative residual refinement for joint optical flow and occlusion estimation. *CVPR*, 2019.
- [13] Vladimir Kolmogorov and Ramin Zabih. Computing visual correspondence with occlusions via graph cuts. Technical report, Cornell University, 2001.

- [14] Florent Lafarge and Clement Mallet. Building large urban environments from unstructured point data. *ICCV*, 2011.
- [15] Richard Lengagne, Pascal Fua, and Olivier Monga. 3D stereo reconstruction of human faces driven by differential constraints. *Image and Vision Computing*, 18(4):337–343, 2000.
- [16] Zhengfa Liang, Yiliu Feng, Yulan Guo, Hengzhu Liu, Wei Chen, Linbo Qiao, Li Zhou, and Jianfeng Zhang. Learning for disparity estimation through feature constancy. *CVPR*, 2018.
- [17] Nikolaus Mayer, Eddy Ilg, Philip Hausser, Philipp Fischer, Daniel Cremers, Alexey Dosovitskiy, and Thomas Brox. A large dataset to train convolutional networks for disparity, optical flow, and scene flow estimation. *CVPR*, 2016.
- [18] Jiahao Pang, Wenxiu Sun, Jimmy SJ Ren, Chengxi Yang, and Qiong Yan. Cascade residual learning: A two-stage convolutional neural network for stereo matching. *ICCV Workshops*, 2017.
- [19] Olaf Ronneberger, Philipp Fischer, and Thomas Brox. U-net: Convolutional networks for biomedical image segmentation. *MICCAI*, 2015.
- [20] Mathias Rothermel, Konrad Wenzel, Dieter Fritsch, and Norbert Haala. SURE: Photogrammetric surface reconstruction from imagery. *LC3D Workshop*, 2012.
- [21] Johannes Lutz Schönberger and Jan-Michael Frahm. Structure-from-motion revisited. *CVPR*, 2016.
- [22] Natalia Slesareva, Andrés Bruhn, and Joachim Weickert. Optic flow goes stereo: A variational method for estimating discontinuity-preserving dense disparity maps. *DAGM*, 2005.
- [23] Schöps T., Schönberger J., Galliani S., Sattler T., Schindler K., Pollefeys M., and Geiger A. A multi-view stereo benchmark with high-resolution images and multi-camera videos. *CVPR*, 2017.
- [24] C. Tomasi and R. Manduchi. Bilateral filtering for gray and color images. *ICCV*, 1998.
- [25] Stepan Tulyakov, Anton Ivanov, and Francois Fleuret. Practical deep stereo (PDS): Toward applications-friendly deep stereo matching. *NeurIPS*, 2018.
- [26] Hoang-Hiep Vu, Patrick Labatut, Jean-Philippe Pons, and Renaud Keriven. High accuracy and visibility-consistent dense multiview stereo. *IEEE TPAMI*, 34(5):889–901, 2011.
- [27] Gengshan Yang, Joshua Manela, Michael Happold, and Deva Ramanan. Hierarchical deep stereo matching on high-resolution images. *CVPR*, 2019.
- [28] Jure Zbontar and Yann LeCun. Stereo matching by training a convolutional neural network to compare image patches. *JMLR*, 17(2):1–32, 2016.

Supplementary Material

In this document, we provide additional details and complementary visualisations that we could not include in the main paper due to space restrictions. In particular,

- we show the full extent of the Zurich dataset and mention further technical details about the model training.
- we show the effect of rectification with the initial surface model, for both the Zurich and ETH3D datasets.
- As a separate file, we provide a video fly-through in which we directly contrast the (median filtered) initial DEM of Zurich with the result of ResDepth refinement for visual comparison.

A. Zurich DEM dataset

The initial DEM is generated with a dedicated satellite stereo pipeline. It covers an area of approximately $1.5 \times 1.5 \text{ km}^2$ with a grid spacing of 0.25 m, corresponding to a total of $\approx 3.7 \cdot 10^7$ pixels. Fig. A2 shows the corresponding ground truth DEM derived from the publicly available 2.5D CAD city model² of Zurich.

We vertically split the area into five mutually exclusive stripes and use three stripes for training, one for validation, and one for testing. The test stripe was chosen to include the full range of buildings (small and large, low and high, residential and industrial), and to avoid regions where the ground truth model is not accurate, particularly around complex bridge structures.

We randomly sample 50'000 patches with 128×128 pixel dimensions (32×32 m in world coordinates) across all three training stripes for training the network. For validation and testing, we use patches cropped in a regular grid of the respective stripe.

B. Image rectification

We show the satellite images used for refining the test region of the Zurich DEM in Fig. A3, 1st and 2nd column. The ortho-rectified counterparts are displayed in the

3rd and 4th column. Note that we deliberately do not perform any ray-casting to account for occlusions during the ortho-rectification process. Instead, we prefer to render duplicate textures if the corresponding rays intersect the surface twice, leading to photometrically inconsistent, systematically displaced copies of nearby textures. This effect is particularly visible for tall buildings.

In Fig. A4, we depict exemplary stereo pairs (1st and 2nd column) of the ETH3D dataset along with the corresponding warped views (3rd column).

C. Video comparison of satellite DEMs

We have included a supplementary video that shows a comparison between the input DEM of Zurich (median-filtered as a realistic, fair baseline) and the ResDepth-*stereo* refinement result. We encourage readers to check out the video, which illustrates the effect of our method much better than small image crops.

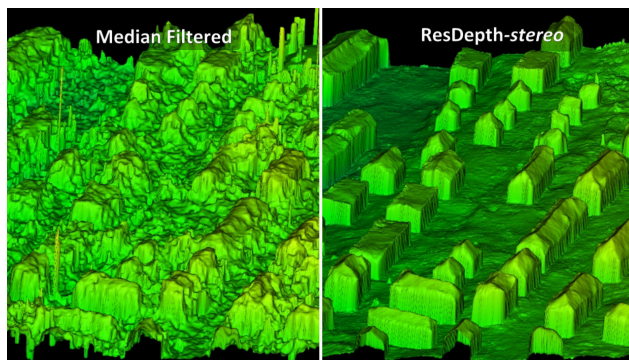


Figure A1. Screenshot from the complementary video fly-through.

²https://www.stadt-zuerich.ch/ted/de/index/geoz/geodaten_u_plaene/3d_stadtmodell.html

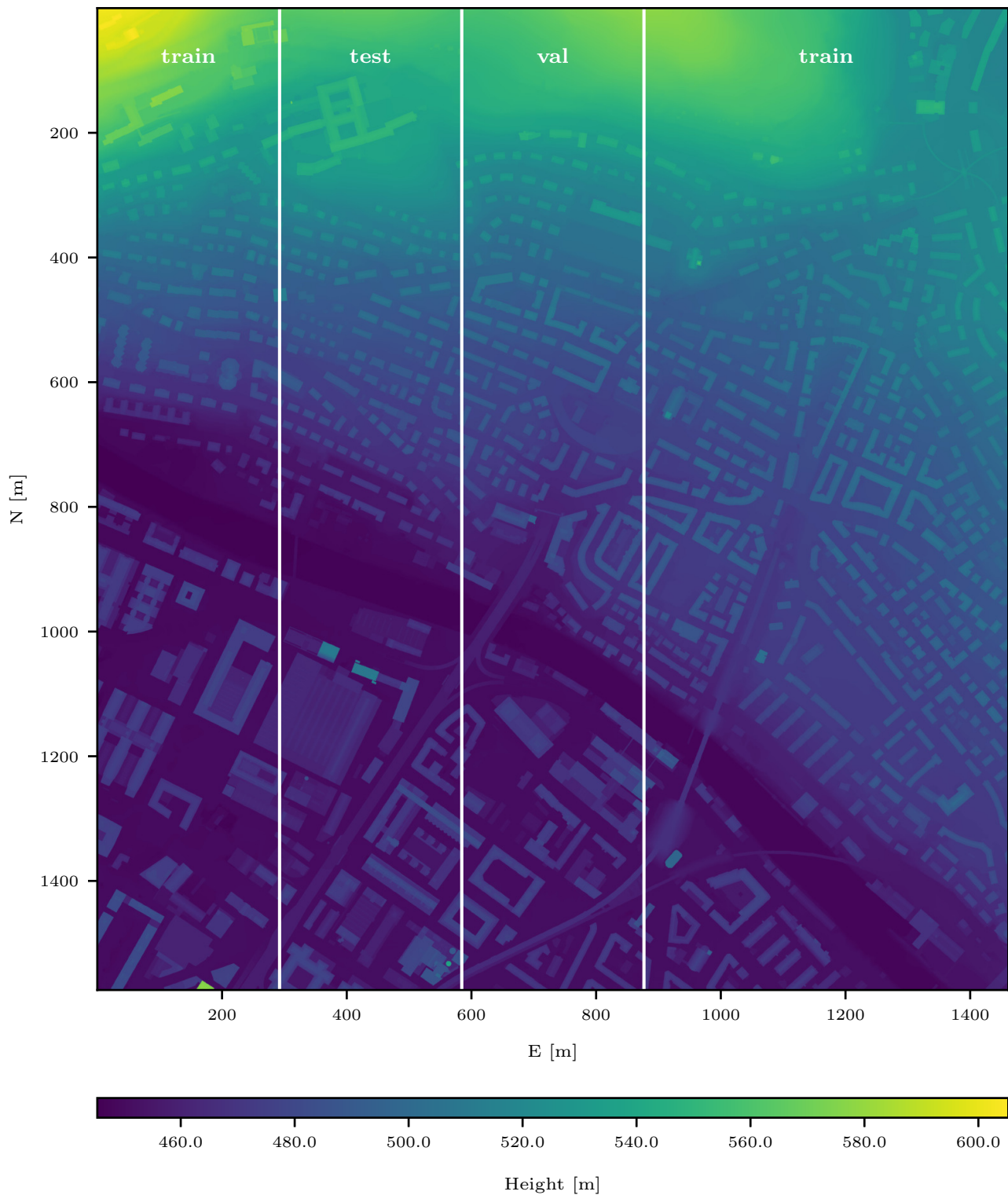


Figure A2. Ground truth DEM of Zurich, separated into training, validation, and test region. The axes show relative coordinates w.r.t. to the upper left corner of the raster DEM. The coordinates of the upper left corner are (463395.0, 5249777.0), given in UTM 32N. The colors indicate ellipsoidal heights (GRS80).

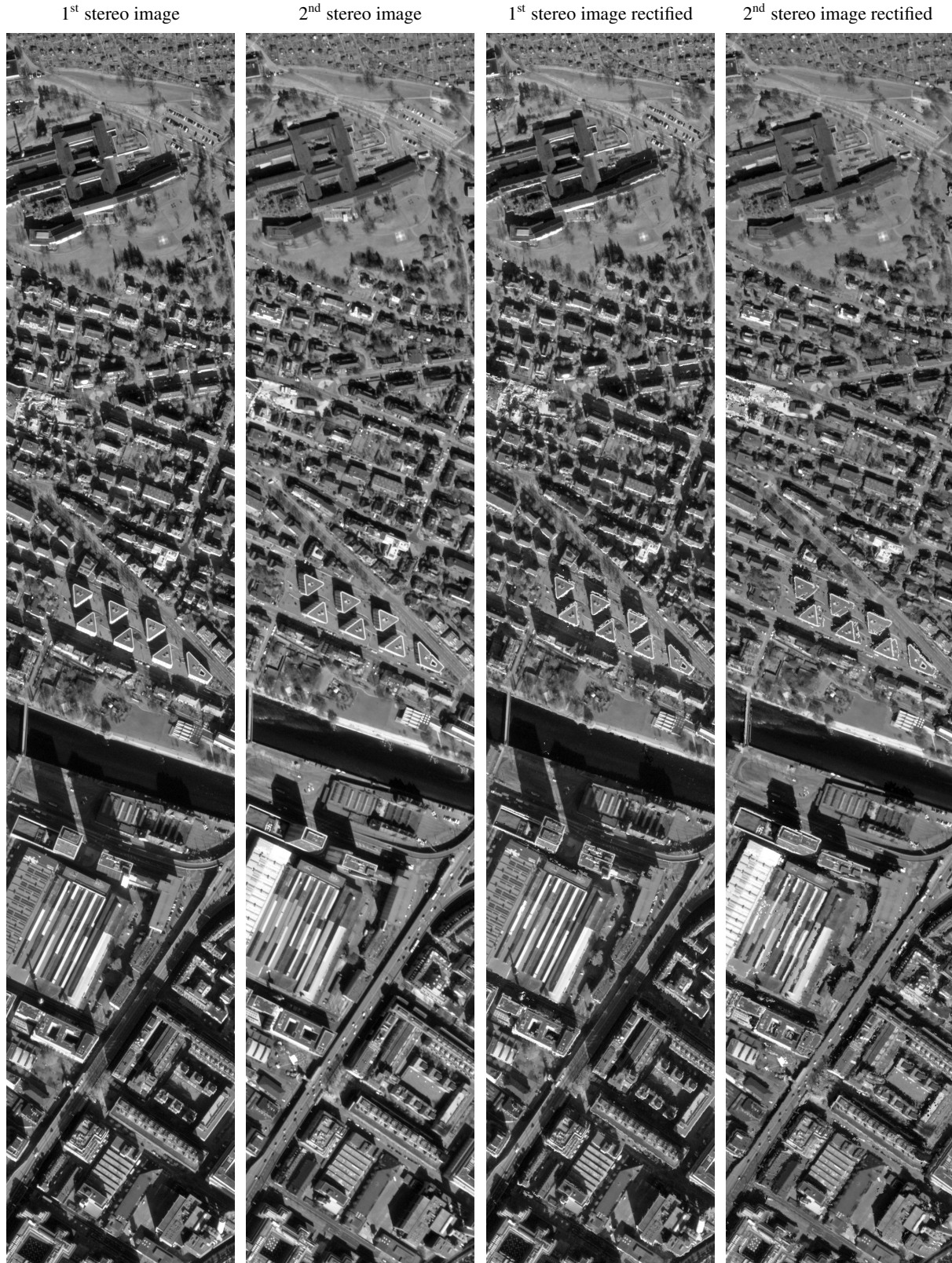


Figure A3. Satellite stereo pair displaying the test region of Zurich. Columns 1-2 show the raw satellite images, columns 3-4 are the ortho-rectified stereo pairs used by the ResDepth network.

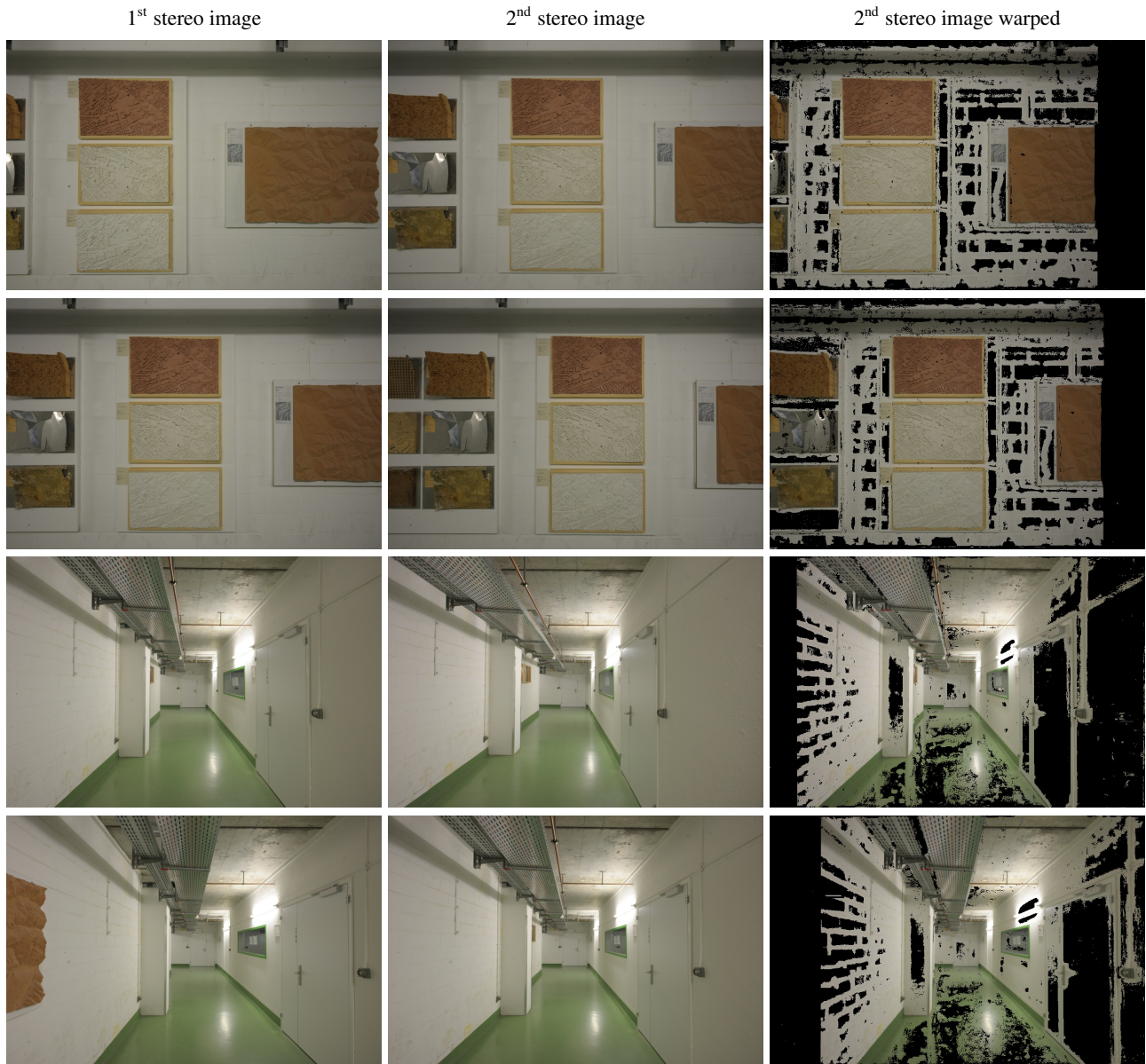


Figure A4. Exemplary stereo pairs from the ETH3D *terrace* scene (part of the test set). Columns 1-2 depict the original views, column 3 shows the 2nd image warped into the reference camera of the 1st image. Pixels without a valid initial depth of the reference camera are displayed in black in the warped view.